.LA-UR -83-2566

CONF-830942--35



LA-UR--83-2566

DE84 001399

TITLE: RADIATION-DAMAGE CALCULATIONS WITH NJOY

AUTHOR(S): R. E. MacFarlane, D. W. Muir, and
F. W. Mann, We    use Hanford Engineering Development Lab.

SUBMITTED TO: The Third Topical Meeting on Fusion Reactor Materials, Albuquerque, New Mexico, September 19-22, 1983

RADIATION-DAMAGE CALCULATIONS WITH NJOY

Robert E. MACFARLANE, Douglas W. MUIR, and F. W. MANN*

Theoretical Division, Los Alamos National Laboratory, Los Alamos, New Mexico, U.S.A.

Atomic displacement, gas production, transmutation, and nuclear heating can all be calculated with the NJOY nuclear data processing system using evaluated data in ENDF/B format. Using NJOY helps assure consistency between damage cross sections and those used for transport, and NJOY provides convenient interface formats for linking data to application codes. Unique features of the damage calculation include a simple momentum balance treatment for radiative capture and a new model for (n, particle) reactions based on statistical model calculations. Sample results for iron and nickel are given and compared with the results of other methods.

## 1. INTRODUCTION

Damage to materials caused by neutron irradiation is expected to be an important design consideration in fusion power reactors. There are many radiation effects that may cause damage, including direct heating, gas production (for example, helium embrittlement), transmutation, and the production of lattice defects. All of these quantities can be calculated easily and consistently using modules of the NJOY nuclear data processing system[1,2] together with evaluated nuclear data from ENDF/B-V.[3]

This paper will concentrate on the calculation of nuclear recoil, which produces the lattice defects. The methods used in the current HEATR module of NJOY will be described, and a new treatment of charged-particle emission will be proposed. Finally, the results will be compared with other radiation damage calculations.

## 2. THE NJOY SYSTEM

The NJOY nuclear data processing system[1,2] processes almost all the types of data given in ENDF/B[3] into the form of continuous-energy or multigroup cross sections for neutrons and photons, and cross-section covariances. The results can be supplied in a variety of formats. Although NJOY is a large system (almost 50 000 card images), it is made simpler by the modular structure sketched in Fig. 1. The RECONR module reconstructs continuous-energy cross sections from ENDF/B resonance parameters and nonlinear interpolation schemes, BROADR is used to Doppler broaden these results, and HEATR is used to add heat-production (kerma) and damage-energy production cross sections. These point-energy ENDF-format results (PENDF) can then be converted to Monte-Carlo format or averaged over energy groups (GROUPR). Not shown are modules for thermal scattering (THERMR), unresolved energy-range cross sections (UNRESR), photon interaction cross sections (GAMINR), covariances (ERRORR), and various input and output formats (MODER, DTFR, CCCCR, MATXSR, POWR, COVR).

With this structure, it is easy to add new information such as heating or damage to the PENDF file. The new data can then be reformatted or group averaged just like any other cross section. Then, the heating and damage numbers can be used for calculations in continuous-energy Monte-Carlo codes such as MCNP[4] or in $S_N$ transport codes such as ONEDANT.[5] Combining the damage calculation with the other cross section processing tasks is convenient, but more importantly, it helps to assure consistency between

*Westinghouse Hanford Engineering Development Laboratory, Richland, Washington, USA.

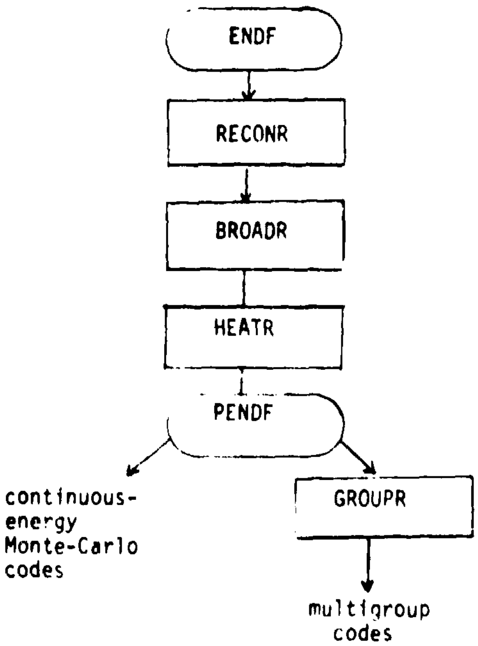


Fig. 1

Simplified structure of the NJOY nuclear data processing system.

the damage and heating cross sections and those used for neutron and photon transport.

3. DISPLACEMENT DAMAGE

A large cluster of lattice defects can be produced by the primary recoil nucleus of a nuclear reaction as it slows down in the lattice. It has been shown that there is an empirical correlation between the number of displaced atoms per lattice atom (DPA) and various properties of metals such as elasticity. The number of displaced atoms depends on the total available "damage" energy $E_a$ and the energy $E_d$ required to displace an atom from its lattice position. Because the available energy is used up producing pairs,

$$DPA = \frac{E_a}{2E_d} \times \frac{\text{neutron collisions}}{\text{lattice atom}} \qquad (1)$$

A wide range of $E_d$ values of 25 to 75 eV is reported in the literature.[6,7] HEATR calculates $E_a$ and multiplies it by the neutron total cross section to obtain the damage-energy production cross section. $E_a$ depends on the recoil energy $E_R$ and the partition of recoil energy between electronic excitations and atomic motion. The partition function used in NJOY was given by Robinson[8] based on the electronic screening theory of Lindhard:[9]

$$P(E) = \frac{E_R}{1 + F_L(3.4008\varepsilon^{1/6} + 0.40244\varepsilon^{3/4} + \varepsilon)}, \qquad (2)$$

if $E_R \geq 25$ eV, and $P(E) = 0$ otherwise. In Eq. (2), $E_R$ is the primary recoil energy and

$$\varepsilon = E_R/E_L \quad , \qquad (3)$$

$$E_L = 30.724\, Z_R Z_L (Z_R^{2/3}+Z_L^{2/3})^{1/2} (A_R+A_L)/A_L \quad , \qquad (4)$$

$$F_L = \frac{0.0793\, Z_R^{2/3}\, Z_L^{1/2}(A_R+A_L)^{3/2}}{(Z_R^{2/3}+Z_L^{2/3})^{3/4}\, A_R^{3/2}\, A_L^{1/2}} \quad , \qquad (5)$$

and $Z_i$ and $A_i$ refer to the charge and atomic number of the lattice nuclei (L) and the recoil nuclei (R). The function behaves like $E_R$ at low recoil energies and then levels off at higher energies. Therefore, the damage-energy production cross section is always less than the heat production cross section. The damage results are suitable for metals only.

At present, recoil energy distributions are not included in the ENDF files, so they have to be estimated using models. For elastic and two-body discrete-level scattering (ENDF/B designations MT=2 and MT=51 through 90), this can be done accurately using

$$E_R(E,\mu) = \frac{AE}{(A+1)^2}(1 - 2M\mu + M) , \qquad (6)$$

where

$$M = \sqrt{1 - \frac{A+1}{A}\frac{(-Q)}{E}} \quad , \qquad (7)$$

and $\mu$ is the center-of-mass scattering cosine. The corresponding damage-energy production cross section is then obtained from

$$D(E) = \sigma(E) \int_{-1}^{1} f(E,\mu)P(E_R[E,\mu])d\mu \quad , \qquad (8)$$

where f is the angular distribution of the scattered neutrons from the ENDF/B File 4. This integration is performed with a 20-point Gauss-Legendre quadrature. Discrete-level reactions with ENDF "LR flags"--for example, $(n,n')\alpha$ reactions--are treated in the same way. The effect of the additional emitted particle on the recoil spectrum is ignored.

Continuum reactions, such as the ENDF MT91 for (n,n'), give a recoil spectrum

$$E_R(E,E',\mu) = \frac{1}{A} (E - 2 \sqrt{EE'} + E') \quad , \qquad (9)$$

where E' is the secondary neutron energy, and $\mu$ is the laboratory cosine. The damage becomes

$$D(E) = \sigma(E) \int_0^\infty dE' \int_{-1}^{1} d\mu \ f(E,\mu) \ g(E \rightarrow E') \times$$

$$P(E_R[E,E',\mu]) \quad , \qquad (10)$$

where g is the secondary-energy distribution from ENDF/B File 5. In HEA.. . the angular distribution is taken to be isotropic, and a four-point Gaussian quadrature is used for the angular integration. For analytic representations of g (see Ref. 3 for details), an adaptive integration to 5% accuracy is used for E'; for tabulated File 5 data, a trapezoidal integration is performed using the energy grid of the evaluation. The same procedure is used for (n,2n), (n,nn), etc., with no account being taken of any extra charged particles emitted.

The treatments used above implicitly neglected the effects of photon momentum; however, this is not a good assumption for radiative capture (ENDF/B MT=102) for incident neutron energies below 25-100 keV. In this case,

$$E_R(E) = \frac{E}{A+1} - 2 \sqrt{\frac{E}{A+1}} \sqrt{\frac{E_\gamma^2}{2(A+1)mc^2}} \cos\phi$$

$$+ \frac{E_\gamma^2}{2(A+1)mc^2} \quad , \qquad (11)$$

where $\phi$ is the angle between the incident neutron direction and the emitted photon direction. If subsequent photons are emitted in a cascade, each one will add an additional term of $E_\gamma^2$ and an additional angle. A complete averaging of Eq. (11) with respect to $P(E_R)$ would be difficult (A Monte-Carlo approach is used in Ref. 7) and would require angular correlations not present in ENDF/B. However, an estimate for the damage obtained by treating the neutron "kick" and all the photon kicks independently should give a conservative upper limit because

$$\int_{-1}^{1} D(E)d(\cos\phi) \le D(\frac{E}{A+1}) + \sum_\gamma D(\frac{E_\gamma^2}{2M_R c^2}) \ . \qquad (12)$$

Finally, the (n,particle) reactions such as (n,p) (MT=103) and $(n,\alpha)$ (MT=107) are computed using

$$E_R = \frac{1}{A+1} (E^* - 2\sqrt{aE^*E_a} \cos\phi + aE_a) \quad , \qquad (13)$$

where a is the mass ratio of the emitted particle to the neutron, E* is given by

$$E^* = \frac{(A+1-a)}{(A+1)} E \quad , \qquad (14)$$

and the particle energy $E_a$ is approximated as being equal to the smaller of the available energy

$$E_{av} = Q + \frac{AE}{A+1} \quad , \qquad (15)$$

or the Coulomb barrier energy

$$E_{cb} = \frac{(1.029 \times 10^6) zZ}{a^{1/3} + A^{1/3}} \quad \text{(in eV)} \quad , \qquad (16)$$

where z is the charge number of the emitted particle and Z is the charge number of the target atom. This "delta-function approximation" has the advantage of avoiding the integration over final energy while still representing the most important feature of the charge-particle spectrum. The angular distribution for the emitted particle is assumed to be isotropic in the lab.

## 4. A NEW TREATMENT OF PARTICLE EMISSION

One possible objection to the NJOY treatment of radiation damage is the "delta function approximation" for particles emitted from (n,p) and (n,α) reactions. Some earlier codes used simple evaporation spectra.[6,7] The DISCS code[10] follows the method of Kikuchi and Kawaii,[11] who employ an energy-shifted evaporation model

$$g(E \to E') = C[E' - K(Z)E_{cb}]$$
$$\exp[-(E' - K(Z)E_{cb})/\theta(E,Z,A)] \quad , \qquad (17)$$

where C is a normalization constant, K(Z) is a function fitted to data, and θ is another fitted function which takes the place of a nuclear temperature. Specifically,

$$\theta(E,Z,A) = \sqrt{\frac{\mu E + Q - E_{cb}}{a(Z,A)}} \quad , \qquad (18)$$

where μ is the reduced mass of the system, Q is the Q values for the reaction, and a is the nuclear level density.

In order to evaluate the relative merits of the various models of particle emission, the Hauser-Feshbach computer code HAUSER*5[12] was used to calculate the outgoing proton and alpha spectra from $n+{}^{27}Al$, $n+{}^{56}Fe$, $n+{}^{58}Ni$, $n+{}^{64}Ni$, $N+{}^{92}Mo$, and $n+{}^{100}Mo$. Very good agreement has been obtained with such calculations and the sparse available experimental data. Using the results for aluminum and iron, a new fitting function was found:

$$g(E \to E') = C[E' - f(Z)]$$
$$\sqrt{E + Q - E} \ \exp[-g(A)E'] \quad , \qquad (19)$$

where

$$f(Z) = 0.1\,Z \quad \text{protons}$$
$$\phantom{f(Z) =} 0.254\,Z \quad \text{alphas} \quad , \qquad (20)$$

and

$$g(A) = -0.072\sqrt{A} \quad . \qquad (21)$$

Figure 2 shows a comparison for $n+{}^{58}Ni$ for 14-MeV incident neutrons. For all the cases studied, the new formula gives good agreement with the calculated values. The new formula also works better than the formula and parameters of Kikuchi and Kawaii, especially for the cases where E+Q is small compared to the Coulomb barrier energy.

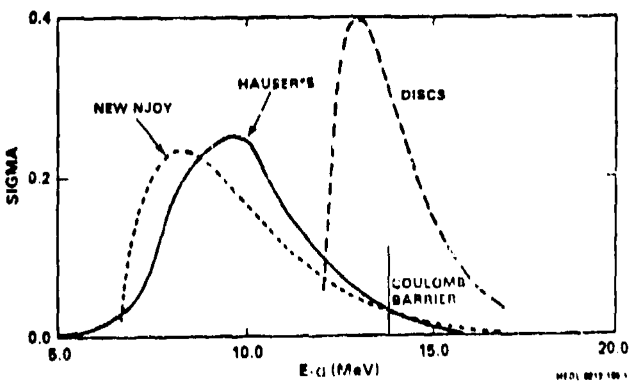


FIGURE 2
Comparison of different models of the α spectrum for the ${}^{58}Ni(n,\alpha)$ reaction.

## 5. COMPARISONS OF RESULTS

A typical total damage-energy production cross section (eV-barns) is shown in Fig. 3. The 1/v behavior at low energies is the photon recoil effect discussed above. The sharp onset of the elastic contribution is due to the 25-ev threshold for Eq. (2). Fig. 4 shows more detail for the high energy range important for fusion. On both graphs, the smooth curves are from NJOY and the (n,particle) absorption reactions were

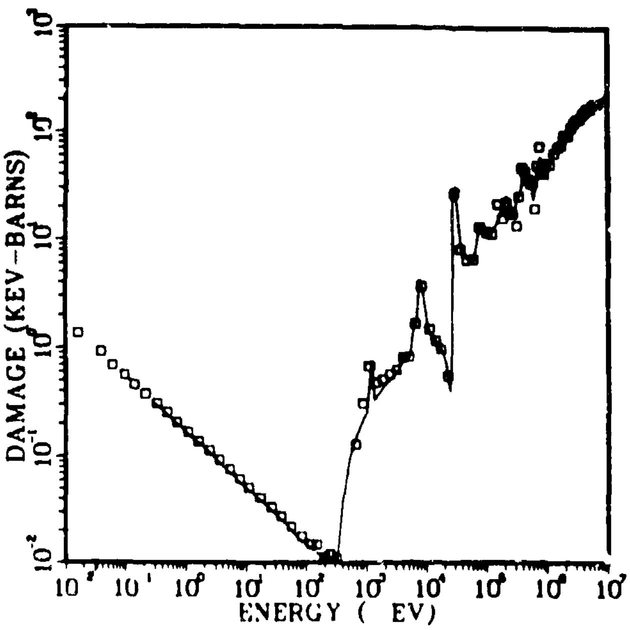


FIGURE 3
Comparison of total damage energy production for iron from "old" NJOY (solid) and DISCS (symbol). Both are multigroup sets plotted at the center of each group.

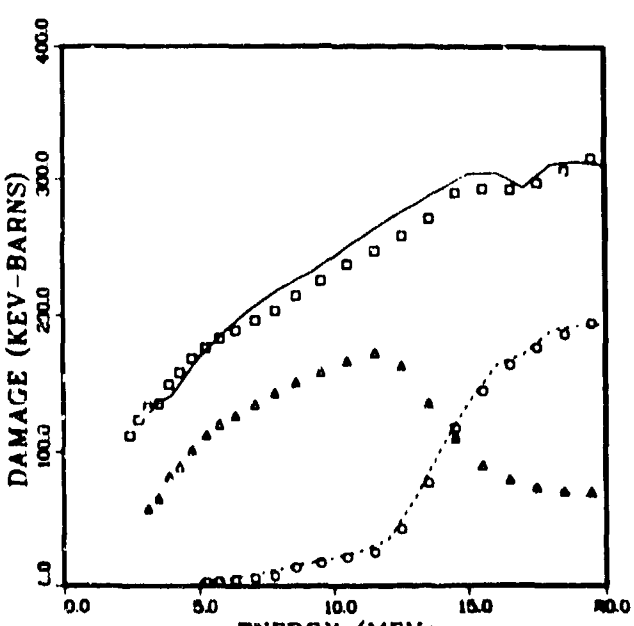


FIGURE 4.
Components of damage energy production for iron at high energies. Curves are results from "old" NJOY, and symbols are values from DISCS[10] (squares are total, triangles are inelastic, and circles are everything but elastic and inelastic).

computed with the old treatment. The points plotted with symbols are multigroup values from the DISCS code[10] and were kindly supplied by L. R. Greenwood of the Argonne National Laboratory.

The effects of the new treatment of particle emission can be seen in Tables I and II. All three methods are in reasonable agreement for (n,p) reactions, but as expected, the new model gives lower results for (n,α) reactions due to the improved treatment of Coulomb barrier penetration. The small effect implies that the initial "kick" given by the neutron capture is more important than the kick from the emitted particle, which sometimes adds to the recoil energy and sometimes subtracts. The large difference for "other" in Table II comes from the (n,n'p) reaction.

TABLE I
Damage Energy Production (keV·barns) for 14-15 MeV Neutrons on Iron

| Reaction | DISCS | Old NJOY | New NJOY |
|---|---|---|---|
| (n,p)+(n,d) | 23.3 | 23.3 | 23.3 |
| (n,α) | 12.3 | 11.6 | 11.2 |
| elastic | 62.3 | 63.5 | 63.5 |
| inelastic | 110.0 | 114.6 | 114.6 |
| other | 82.1 | 85.8 | 85.8 |
| total | 290.0 | 298.8 | 298.4 |

TABLE II
Damage Energy Production (keV·barns) for 14-15 MeV Neutrons on Nickel

| Reaction | DISCS | Old NJOY | New NJOY |
|---|---|---|---|
| (n,p)+(n,d) | 41.6 | 51.9 | 52.0 |
| (n,α) | 47.9 | 45.2 | 43.9 |
| elastic | 62.3 | 63.4 | 63.4 |
| inelastic | 64.7 | 58.3 | 58.3 |
| other | 83.5 | 48.5 | 48.4 |
| total | 300.0 | 267.3 | 266.0 |

. .

## 6. CONCLUSIONS

The NJOY system provides a convenient way to compute damage cross sections or DPA that are consistent with the heating, transmutation, gas production, and transport cross sections used for a particular analysis. The results compare well with those of other codes, and provide significantly improved results for high-energy capture reactions.

Remaining shortcomings include the neglect of recoil effects from charged particles in three- and four-body reactions, and the neglect of preequilibrium effects on the angular distributions of emitted particles. These effects are being attacked with a completely new approach for adding evaluated recoil spectra to the ENDF/B files.[13]

The NJOY system is available through the National Energy Software Center at the Argonne National Laboratory, the Radiation Shielding Information Center at the Oak Ridge National Laboratory, and the European NEA Data Bank at Saclay, France. Several prepocessed libraries in MATXS format are available on the Magnetic Fusion Energy Computer Center network, and the damage cross sections can be easily formatted for transport codes using TRANSX-CTR.[14]

## REFERENCES


1. R. E. MacFarlane, D. W. Muir, and R. M. Boicourt, "The NJOY Nuclear Data Processing System, Volume I: User's Manual," Los Alamos National Laboratory report LA-9303-M (ENDF-324) (May 1982).

2. R. E. MacFarlane, D. W. Muir, and R. M. Boicourt, "The NJOY Nuclear Data Processing System, Volume II: The NJOY, RECONR, BROADR, HEATR, and THERMR Modules," Los Alamos National Laboratory report LA-9303-M (ENDF-324) (May 1982).

3. R. Kinsey, "ENDF-102 Data Formats and Procedures for the Evaluated Nuclear Data Files, ENDF," Brookhaven National Laboratory report BNL-NCS-50496 (ENDF-102) 2nd Ed. (ENDF/B-V) (1979).

4. "MCNP-A General Monte Carlo Code for Neutron and Photon Transport," Los Alamos National Laboratory report LA-7396-M, Revised (Nov. 1979).

5. R. D. O'Dell, F. W. Brinkley, Jr., and D. R. Marr, "User's Manual for ONEDANT:A Code Package for One-Dimensional Diffusion-Accelerated Neutron-Particle Transport," Los Alamos National Laboratory report LA-9184-M (Feb. 1982).

6. T. A. Gabriel, J. D. Amburgy, and N. M. Greene, "Radiation-Damage Calculations: Primary Knock-On atom Spectra, Displacement Rates, and Gas Production Rates," Nucl. Sci Eng. 61, 21 (1976).

7. D. G. Doran, "Neutron Displacement Cross Sections for Stainless Steel and Tantalum Based on a Linhard Model," Nucl. Sci. Eng. 49, 130 (1972).

8. M. T. Robinson, in Nuclear Fusion Reactors (British Nuclear Energy Society, London, 1970).

9. J. Lindhard, V. Nielsen, M. Scharff, and P. V. Thomsen, Kgl. Dansk, Vidensk, Selsk, Mat-Fys. Medd. 33 (1963).

10. R. K. Smither and L. R. Greenwood, "Displacement Damage Calculations using ENDF/B-V Cross Sections Including Thermal Neutron Capture and Beta Decay Effects," Proc. of 4th ASTM-Euratom Sym. on Reactor Dosimetry, EUREG/CP-0029, p. 793.

11. K. Kikuchi and M. Kawaii, Nuclear Matter and Nuclear Reactions, p. 135 (1968)

12. F. M. Mann, "HAUSER*5, A computer Code to Calculate Nuclear Cross Sections," HEDL-TME-78-83 (July 1979).

13. R. E. MacFarlane and D. G. Foster, Jr., "Advanced Nuclear Data for Radiation Damage Calculations," Proc. of Third Topical Meet. on Fusion Reactor Materials, Albuquerque, New Mexico, Sept. 12-22, 1983 (to be published).

14. R. E. MacFarlane, "TRANSX-CTR, A Code for Interfacing MATXS Cross-Section Libraries to Nulcear Transport Codes for Fusion Systems Analysis," Los Alamos National Laboratory report LA-9863-MS (1983).